Nitrate radical chemistry over the sub-Arctic Pacific

Nicole Mölders[*1,2], Trang T. Tran[2,3], Greg Newby[3], W.R. Simpson, W.R. Stockwell[4]

[1]University of Alaska Fairbanks, Geophysical Institute, [2]University of Alaska Fairbanks, College of Natural Science and Mathematics, Department of Atmospheric Sciences, [3]Arctic Region Supercomputing Center, [4]Howard University

1. Introduction

In mid-latitudes, nocturnal chemistry and physics strongly affect the nitrogen oxides (NO_x=NO+NO_2 nitric oxide, nitrogen dioxide) budget and consequent production of ozone (O_3; Brown et al. 2004). A large fraction of NO_2 forms nitrate radicals, NO_3, and dinitrogen pentoxide, N_2O_5 during the night. The variability in N_2O_5 chemistry can lead to either strong or weak sinks for NO_x (Brown et al. 2004). Tropospheric N_2O_5 permits reversible, temperature-dependant storage and/or transport of NO_x. It hydrolyzes readily to nitric acid (HNO_3) via a heterogeneous reaction on the surface of aerosol particles, a potentially efficient NO_x sink. NO_3 can react with reduced sulfur compounds and hydrocarbons to produce HNO_3.

During daytime photolysis and the presence of NO efficiently destructs NO_3. Because NO_2 is photolyzed to form O_3, NO_x repartitions to notable amounts of NO. Some of the NO destroys NO_3 and limits NO_3 and N_2O_5. Often NO is more a limiting factor for daytime NO_3 and N_2O_5 than NO_3 photolysis. NO also reacts with free radicals from photolysis of volatile organic compounds (VOC). These free radicals recycle NO to NO_2. This means that each molecule of NO can produce O_3 multiple times until the VOC chains of carbon compounds are too short to be photolyzed. Over the ocean, the main VOC source is from ship emissions. In mid-latitudes, the reaction of NO_2 with photochemically-produced OH produces HNO_3 and accounts for the majority of NO_x loss during the day (Brown et al. 2004).

In mid-latitudes, peroxyacetyl nitrates (PANs) formation is a significant instantaneous NO_2 loss, but not a long-term NO_x sink. A source of peroxy radicals is the thermal decay of photochemically-produced PAN that can persist into the night. In the sub-Artic, however, PAN becomes subject to long-range transport (Moxim et al. 1996) even in the atmospheric boundary layer (ABL) and serves as a long-term reservoir for NO_x (Mölders et al. 2010). Under certain atmospheric conditions (T<263K), NO_3 can be a more important sink for polycyclic aromatic hydrocarbons (PAH) than NO_2, HNO_3, N_2O_5, or O_3 after long NO_3 exposure times. In the sub-arctic winter, temperatures are typically lower than this threshold.

In mid-latitudes, ozone concentrations decrease towards the surface and are about 40ppb in the upper nocturnal boundary layer (NBL). The positive O_3-gradient results from dry deposition and titration with NO emitted close to the ground. NO_2 often develops a negative vertical gradient due to production by reactions of NO with O_3. The vertical profiles of N_2O_5 depend strongly on those of NO_3, NO_2 and temperature (Geyer and Stutz, 2004).

This paper examines the fate of NO_3 and N_2O_5 as either a reservoir or a sink for NO_x over the sub-Arctic Pacific in January. In subarctic and Arctic winter, hardly any daylight and photochemistry exist. Radiative cooling suppresses convection and often generates stable vertical stratification. The negative buoyancy reduces the vertical transport produced by wind shear. Inversions over the sub-Arctic Pacific (Bering Sea, Gulf of Alaska) may trap the pollutants emitted along sea routes. Characterization of the nocturnal processes is critical to understanding the cycling of NO_x in sub-Arctic winter.

2. Experimental design

We used WRF/Chem with the following model setup: Cloud microphysical processes were treated with Lin et al.'s (1983) bulk-parameterization scheme that considers cloud-water, rainwater, cloud-ice, snow, graupel and hail. Grell and Dévényi (2002) cumulus ensemble scheme was applied for convection. Long-wave and shortwave radiation were considered by the Rapid Radiative Transfer Model (RRTM; Mlawer et al. 1997) and the Goddard shortwave scheme, respectively. Viscous sub-layer and ABL processes were dealt with by the similarity scheme and the Mellor-Yamada-Janjic scheme of the Eta model. The exchange of heat, and moisture at the atmosphere-surface interface was calculated by the NOAH land-surface model (Chen and Dudhia 2000). NOAH predicts soil temperature and moisture states at four depths, canopy moisture and snow-cover. Fractional sea-ice was considered.

Atmospheric chemistry reactions were described by the Regional Acid Deposition Model version 2 (RADM2; Stockwell et al. 1990). Inorganic reactions and constants involve 14 stable inorganic compounds, four inorganic short-lived intermediates and three abundant stable species (oxygen, nitrogen, water). The organic chemistry scheme considers 26 groups of stable organic compounds and 16 groups of organic short-lived intermediates (peroxy radicals). Photolysis calculation considered 21 photo-chemical reactions (Madronich 1987).

We used the Modal Aerosol Dynamics Model for Europe (MADE; Ackermann et al. 1998) to simulated aerosol physics and chemistry and aqueous reactions. The Secondary Organic Aerosol Model (SORGAM; Schell et al. 2001) was applied to simulate secondary organic aerosols. Sea-salt properties was calculated as a function of wind speed.

Wesley's (1989) dry deposition module was modified in accord with (Zhang et al. 2003) to treat dry deposition of trace gases more realistically at low temperatures as they occur in Siberia and Alaska during January. Since the stomata of boreal forest are still open at -5°C, the threshold for total closure of stomata was lowered accordingly. Alaska-typical vertical profiles of background concentrations were used (Mölders et al. 2010).

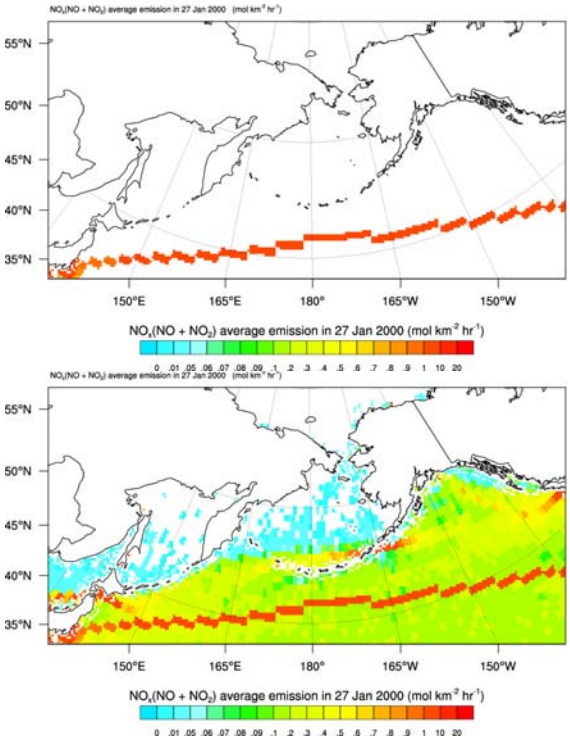

Fig. 1. Average ship emission of NO_x for 1-27-2000 from international ship traffic derived from EDGAR (top) and average ship emissions as obtained from the combined data from EDGAR and RETRO (bottom).

Anthropogenic emissions for 2000 were derived from the Emission Database for Global Atmospheric Research (EDGAR) that provides annual emission inventories on a 1°×1° grid. It considers fossil-fuel related sources, bio-fuel combustion, industrial production and consumption processes including solvent use and landuse-related sources including waste treatment. Since EDGAR only includes the international ship emissions, the domestic ship emissions are taken from the REanalysis of the TROpospheric (RETRO) to account for the total ship emissions (Fig. 1). This dataset has a 1°×1° and monthly resolution for domestic ship emissions. To obtain hourly emission data allocation functions for the month, day-of-the-week and hour were used (Wang et al. 2007, Mölders 2009). The VOC and NMVOCs split follows Theloke and Friedrich (2007) for all anthropogenic emissions except from ships that follows Eyring et al. (2005).

Biogenic emissions of isoprene, monoterpenes, and other VOCs from vegetation and nitrogen from the soil were caclulated inline in accord with Guenther et al. (1994) and Simpson et al. (1995).

The model domain encompasses the atmosphere over the North Pacific (centered at 59°N, 179°E) from East Asia to western Canada (Fig. 1) with 240×120 grid points and a horizontal grid increment of 30km and 27 vertical layers that increase with height.

The National Center for Atmospheric Research and National Centers for Environmental Prediction $1^o \times 1^o$ and six-hour resolution global final analysis (FNL) data served as initial and boundary conditions for meteorological quantities.

At the beginning of the simulation, the chemical fields were initialized using typical Alaska background concentration (Mölders et al. 2010). The chemical fields of the previous simulation were used as initial conditions for the next simulation of the following day. The meteorological conditions were initialized every 5 days.

3. Preliminary results

The cyclones that occur frequently over the northern Pacific during the episode of interest take up pollutants from emissions in Asia and along the international sea routes transporting pollution to the sub-Arctic Pacific and Alaska. Secondary pollutants form during transport. The long nights affect atmospheric chemistry.

NO_2 is less than 0.01ppb in northern Siberia, the Chukchi Sea and northern Alaska in areas that do not receive any insolation. NO_2 concentrations exceed 5ppb over the Asian industrial centers, and Seattle and Vancouver that have large ports. Along the warm fronts of cyclones that moved over these industrial centers and/or sea routes, concentrations are around 0.5 and locally exceed 1ppb.

In areas that receive insolation, NO_x shows a diurnal cycle with higher concentrations at day than night. Phase and amplitude depend on the duration and intensity of insolation. NO_x is highest in the surface layer and decreases rapidly with height. At 2km, average NO_x concentrations are more than an order of magnitude smaller that close to the surface.

In areas that do not receive any solar radiation at all within 24h, NO_3 concentrations range between 0.01 and 0.05ppt all the time. However, this area without insolation decreases as days get longer later in January. Southward of this area, NO_3 goes down to less than 0.01ppt during the day and builds up as night falls. Typically, values are around 0.05ppt during the night, but locally increase as cyclones take up pollutants from the sea routes and/or from Asia. Over the Asian industrial areas, nighttime NO_3 concentrations are around 5ppt, but locally exceed 10ppt. In cyclones that passed the Asian industrial centers and/or sea routes, NO_3 reaches up to 5ppt. On average, NO_3 decreases with height. At 2.5km, NO_3 concentrations are typically about half their near-surface values.

North of 65°N, N_2O_5 concentrations exceed 0.05ppt most of the time. During hours without solar radiation N_2O_5 exceeds 50ppt over the Asian industrial centers and ranges between 5 and 10ppt over the sea routes. If a cyclone takes up polluted air from Asia and/or the sea routes, N_2O_5 concentration will show the pattern of the cyclone when there is no insolation. As solar radiation increases, N_2O_5 is destroyed and approaches zero. During the next night, N_2O_5 will form again and depict the cyclone's pattern, but with lower concentrations than the night before until the cyclone decays. In these cyclones, N_2O_5 concentrations locally exceed 10ppt and typically range between 0.1 and 5ppt. N_2O_5 concentrations are highest in the surface layer and decrease with height. Typically, N_2O_5 concentrations are an order of magnitude or more smaller at 2km height than at the surface.

In areas with solar radiation, NO_3 and N_2O_5 show distinct diurnal cycles (Fig. 2). NO_3 formation starts earlier and destruction starts later than for N_2O_5. As January progresses the amplitude of the diurnal NO_3 cycle slightly decreases on average. In areas with low duration of insolation, the diurnal cycle hardly exists. Obviously, during the dark nights advection of polluted air governs NO_3 and N_2O_5 concentrations. In areas with insolation, the diurnal cycle governs the NO_3 and N_2O_5 and peak concentrations are slightly affected by advection of polluted air.

HNO_3 concentrations are around 0.05ppb except for China and Japan, and in fronts. Over the Asian industrial centers, HNO_3 concentrations amount ~5ppb. Cyclones take the HNO_3 burdened air onto Pacific. In fronts, HNO_3 concentrations amount between 0.1 and 0.5ppb. Ahead of the fronts, HNO_3 concentrations are less than 0.001ppb.

The HNO_4 concentrations show a distinct diurnal cycle. North of 70°N HNO_4 concentrations exceed 0.1ppt most of the time, but locally sometimes exceed 1ppt. In the downwind of the Asian industrial centers, HNO_4 concentrations exceed 10ppt the entire time, while these concentrations are exceeded occasionally in the downwind of the sea routes.

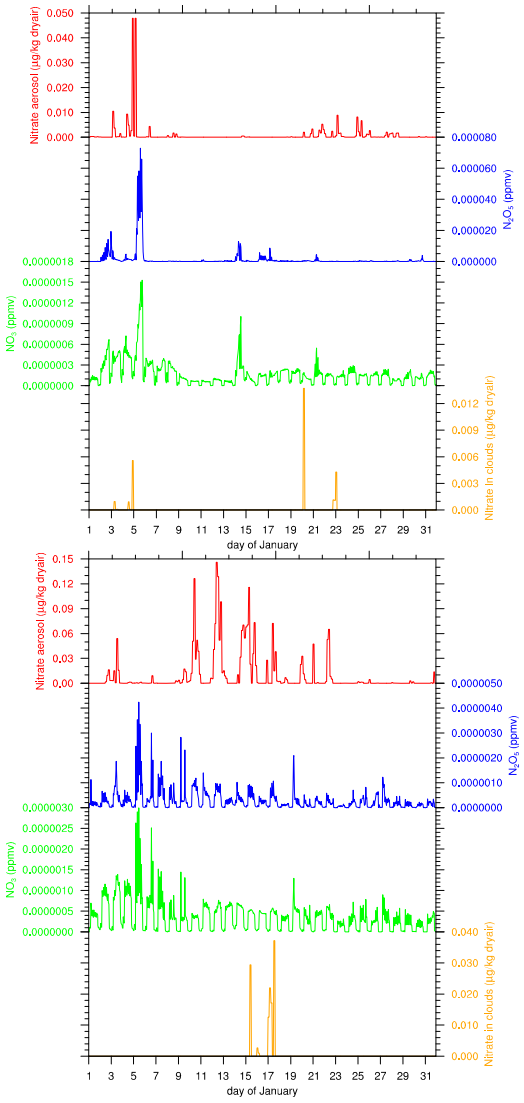

Fig. 2. Time series near-surface NO_3, N_2O_5, nitrate aerosol and nitrate in clouds at 61.97N, 148.26W (Bering Sea, top), and 47.96N, 177.32E (middle of North Pacific, bottom) Nitrate concentration in cloud is zero if no fog exists or only ice fog occurs.

In the area of the Asian industrial centers, daylight hours are long enough to permit for PAN formation. Cyclones transport PAN onto the Pacific to the subarctic Pacific and Alaska. PAN concentrations are highest in the cold sector of cyclones (~0.3ppt or higher). As the cyclones move north, ambient air becomes relatively cooler than farther south for which lifetime of PAN increases. Thus, PAN concentrations are high over the subarctic and Alaska. As PAN-loaden air moves south, PAN decreases in re-

sponse to increasing temperature due to thermal decomposition into NO_x (Fig. 3). Subsequently, NO_x concentrations increase.

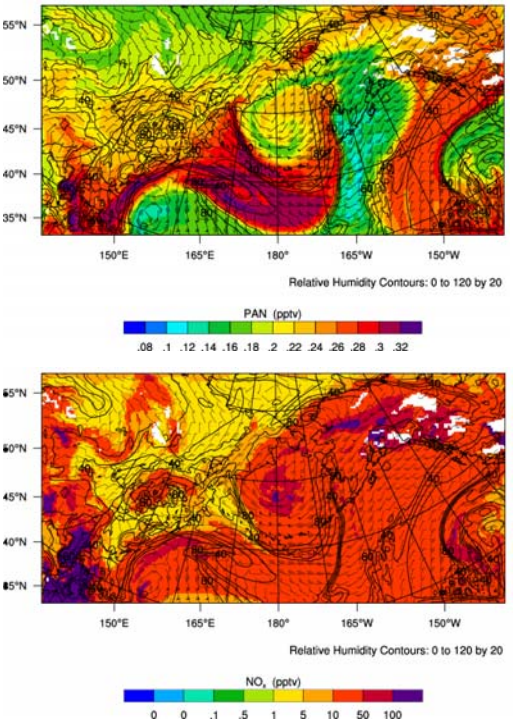

Fig. 3. Simulated PAN (top) and NO_x concentrations at 850hPa for January 18 2000UTC.

NO titrates O_3. Ozone concentrations are around 40ppb most of the time with higher concentrations in cloud-free areas and at low than high latitudes. In polluted air, NO_x locally titrates O_3 to below 20ppb. Eventually, as this NO_x dilutes with background air downwind, the ozone becomes the more available species.

In the Aitken mode, NO_3 aerosol concentrations (nitrate anion NO_3^-) and nitrate in clouds (nitrate radical) are more than an order of magnitude higher ahead of fronts than elsewhere. In the accumulation mode, NO_3 aerosol concentrations and nitrate in clouds are high in the warm sector of cyclones. NO_3 aerosol concentrations are reduced in cloudy areas as compared to adjacent cloud-free areas. On average, NO_3 aerosol and nitrate in cloud concentrations show a slight diurnal sensitivity. In clouds, nitrate is highest in the lower ABL around 400m above NSL. Above 2km height, hardly any nitrate exists in clouds. Nitrate in clouds shows a distinct diurnal cycle with a maximum around 1600 UTC (end of night in the southern part of the domain). Nitrate aerosol concentrations show a slight diurnal sensitivity with higher concentrations at night. They are highest close to the surface and decrease with height. From the surface to 250m above NSL they decrease by more than half. Above 1.5km average nitrate aerosol concentration falls below $1.5 \cdot 10^{-3} \mu g / m^3$.

Acknowledgements

We thank C.F. Cahill, G. Kramm, and H.N.Q. Tran for fruitful discussion. This research was in part supported by NSF under ATM-0926220 and a grant of HPC resources from the ARSC at UAF as part of the DoD HPC Modernization Program.

References

Ackermann, I.J., et al. 1998: *Atmos. Environ.* **32,** 2981-2299.

Brown, S.S., et al., 2004: *Geophys. Res. Lett.*, **31,** L07108.

Chen, F. and J. Dudhia, 2000: *Mon. Wea. Rev.*, **129,** 569–585.

Chou, C.C.-K., et al. 2009: *J. Geophys. Res.*, **114,** D00G01, doi:10.1029/2008JD010446.

Eyring, V., et al. 2005: *J. Geophys. Res.*, **110,** D17306.

Geyer, A. and J. Stutz, 2004: *J. Geophys. Res.*, **109,** D12307.

Grell, G.A. and D. Dévényi, 2002: *Geophysical Research Letters*, **29**.

Guenther, A., et al. 1994: *J. Geophy. Res.*, **100D,** 8873-8892.

Lin, Y.-L. et al., 1983: *J. Appl. Meteor.* , **22,** 1065-1092.

Madronich, S., 1987: *J. Geophys. Res.*, **92,** 9740-9752.

Mlawer, E.J. et al. 1997: *J. Geophys. Res.*, **102D,** 16663-16682.

Mölders, N., 2009: Alaska Emission Model (AkEM) description, 10 pp.

Mölders, N., et al. 2010: *Atmos. Environ.*, **44,** 1400-1413.

Moxim, W.J. et al. 1996: *J. Geophys. Res.*, **101,** 12621-12638.

Schell, B. et al. 2001: *J. Geophys. Res.*, **106,** 28275-28293.

Simpson, D., et al. 1995: *J. Geophys. Res.*, **100D,** 22875-22890.

Stockwell, W.R. et al. 1990: *J. Geophys. Res.*, **95,** 16343-16367.

Theloke, J. and R. Friedrich, 2007: *Atmos. Environ.*, **41,** 4148–4160.

Wang, C., et al. 2007: *Environ. Sci. Technol.*, **41,** 3226-3232.

Wesley, M.L., 1989: *Atmos. Environ.* **23,** 1293-1304.

Zhang, L. et al. 2003: *Atmos. Chem. Phys.*, **3,** 2067-2082.